Journal of Materials Chemistry C

PAPER

View Article Online
View Journal | View Issue

Cite this: J. Mater. Chem. C, 2014, 2, 2089

Large area solution processed transparent conducting electrode based on highly interconnected Cu wire network†

S. Kiruthika, Ritu Gupta,* K. D. M. Rao, Swati Chakraborty, Nagarajan Padmavathy and Giridhar U. Kulkarni*

Received 2nd November 2013
Accepted 10th December 2013

DOI: 10.1039/c3tc32167c

www.rsc.org/MaterialsC

Virtually unlimited and highly interconnected Cu wire networks have been fabricated on polyethylene terephthalate (PET) substrates with sheet resistance of <5 Ω □$^{-1}$ and transmittance of ~75%, as alternatives to the commonly used tin doped indium oxide (ITO) based electrodes. This is a four step process involving deposition of commercially available colloidal dispersions onto PET, drying to induce crackle network formation, nucleating Au or Pd seed nanoparticles inside the crackle regions, washing away the sacrificial layer and finally, depositing Cu electrolessly or by electroplating. The formed Cu wire network is continuous and seamless, and devoid of crossbar junctions, a property which brings high stability to the electrode towards oxidation in air even at 130 °C. The flexible property of the PET substrate is easily carried over to the TCE. The sheet resistance remained unaltered even after a thousand bending cycles. The as-prepared Cu wire network TCE is hydrophobic (contact angle, 80°) which, upon UV–ozone treatment, turned to hydrophilic (~40°).

Introduction

With the developments in optoelectronics during last few decades, indium tin oxide (ITO) has become the most suitable transparent conducting material in optoelectronic devices, namely solar cells,[1] displays,[2] organic light emitting diodes[3] and touch screens.[4] There are, however, some critical issues associated with ITO related to its mechanical stability, high temperature and chemical stability and brittleness.[5–7] The increasing price of In is indeed prohibitive for large area applications. Although many oxide formulations such as Cu_2O, CuS, PbO and Al or Ga doped ZnO, have been developed by physical and solution based processing,[8] these alternative oxides are still not able to meet the required standards of a transparent conducting electrode (TCE) in terms of the sheet resistance (10 Ω □$^{-1}$) and transmittance (~90%), as does ITO.

In the last few years, there have been several new generation TCEs based on nanomaterials such as graphene films,[9,10] carbon nanotube (CNT)[11–14] and metal nanowire networks,[15–17] and nanofibers[18] as well as thin metal films.[19] Although carbon as a material is inexpensive and abundant, the process of conversion to useful forms, CNTs or graphene, is highly energy intensive and the cost is prohibitive, particularly for large area applications.[20] Often, physical deposition methods from the vapour phase are involved, which could be time consuming and expensive. On the other hand, Ag nanowires can be produced in large quantities by simple solution processing,[17] but Ag as a material is scarce and expensive. The best alternative would be to use a cheaper metal such as Cu without much compromise in other factors. Copper has a resistivity of 1.59 nΩ m (Ag, 1.67 nΩ m) and is abundant (1000 times the abundance of Ag).[21] There has been some effort in the literature towards TCE fabrication using Cu in the form of grating structures, either by physical deposition[22] or through a solution route.[23] The other methods include electrospun fibres[15,18,24] or solution dispersed Cu nanowires.[25–31] Zhang *et al.*, for example, developed a novel recipe for synthesizing ultra long single crystalline Cu nanowires and dispersing them over a transparent substrate.[26] The nanowire based electrodes, in general, suffer from junction resistance and the situation is even worse with Cu due to its surface being highly reactive.[27] A Cu nanowire TCE can become oxidised in ambient operation, giving it a very high sheet resistance.[28] Kholmanov *et al.* synthesized Cu-graphene hybrid electrodes to prevent oxidation of Cu nanowires.[29] Meanwhile, Rathmell *et al.* covered the Cu fibres with PVA to prevent the surface oxidation,[30,31] Hsu *et al.* performed atomic layer deposition of aluminium zinc oxide and passivated the surface of Cu

Chemistry & Physics of Materials Unit and Thematic Unit of Excellence in Nanochemistry, Jawaharlal Nehru Centre for Advanced Scientific Research, Jakkur P.O., Bangalore, 560064, India. E-mail: kulkarni@jncasr.ac.in; ritu.jnc@gmail.com

† Electronic supplementary information (ESI) available: Fig. S1–S9, uniform distribution of crackle over large area (Fig. S1), SEM images of dried CP-1 and CP-2 dispersion (Fig. S2), variation in crackle width (Fig. S3), XRD and transmittance of Cu network TCE (Fig. S4 and S5), characterization of Pd seed layer (Fig. S6), transmittance spectrum of Cu network with different wire widths (Fig. S7), SEM image showing non-specific deposition of Cu by solution processing (Fig. S8), schematic and transmittance spectrum of Cu network prepared by physical deposition (Fig. S9). See DOI: 10.1039/c3tc32167c

nanofibers.[27] While passivating nanowire surface should enhance stability, the root cause appears to be the junction resistance which triggers the oxidation process.[32] We considered it important to address this issue and have therefore explored a method of producing Cu TCE with seamless junctions, importantly, through solution processing. Here, a dried colloidal layer hosting a continuous network of cracks serves as a template for Cu deposition through solution processing. The TCEs produced exhibit high transmittance (~75%) and low sheet resistance (<5 Ω $\square^{-1}$) and are highly stable under ambient operation.

Results and discussion

A colloidal dispersion upon drying on a substrate tends to crack due to the stress induced by solvent evaporation.[33] A well-formed crack pattern may be in the form of a network with crack regions exposing the substrate surface underneath, which we term as a crackle network. The crackle network template is highly scalable and based on the colloidal particle size, concentration of the dispersion and the template thickness, a crackle network of a given length scale can be achieved over large areas with a high degree of uniformity (ESI, Fig. S1†). We have produced crackle networks of two different length scales, using two crackle dispersions, both are inexpensive and available commercially.

The CP-1 dispersion, which is essentially a dispersion of SiO_2 nanoparticles (~20 nm, see ESI, Fig. S2†), is available as a wall paint while CP-2 is an acrylic resin (~50 nm, ESI, Fig. S2†). In each case, the concentration of the crackle dispersion was optimized in such a way that upon drying, it resulted in a dried layer hosting highly interconnected cracks. The crackle dispersions were pipetted on polyethylene terephthalate (PET) substrates and spread over the surface using a Mayer rod coater (Fig. 1a). First, it resulted in a wavy wet layer of thickness ~45 μm which settled into a smooth and uniform film as the solvent evaporated in few seconds. As drying continued, a crackle network appeared spontaneously (Fig. 1b and c) due to the internal stresses in the film. Under the given experimental conditions, CP-1 produced cracks with widths in the range of 50–100 μm while CP-2 gave rise to much finer cracks (~4–8 μm). Moreover, the crackle width can be altered by optimizing the concentration of the CP dispersion (see ESI, Fig. S3†). In both cases, the cracks went deep down to the substrate surface (see insets in Fig. 1b and c). These crack patterns were exploited as sacrificial templates for the site selective deposition of Cu metal.

Selective deposition of Cu in the crackle regions was achieved by first depositing Pd or Au catalyst particles over the dried template (Fig. 2a). As ultralow quantities of the noble metal catalyst are required for Cu deposition, the additional cost of catalyst per unit area of the substrate is rather low (see ESI, note S1†). The CP-1 and CP-2 substrates were dosed with Pd by dipping the substrate carrying the crackle template in $PdCl_2$ solution (3 mM in ethylene glycol) and heating to 120 °C for 30 min to nucleate Pd catalyst particles. Alternatively, Au sputtering was also used for seeding the catalyst particles. Au sputtering is considered highly applicable for roll-to-roll coating,[34] unlike other physical methods. The crackle layer was then washed away with acetone (CP-1) or chloroform (CP-2) to leave catalyst particles in the crackle network pattern on the substrate as shown in Fig. 2b. This was followed by electroless and electroplating deposition of Cu to the desired thickness (see Experimental section for details).

The process of Cu deposition on Au seed particles in the CP-1 crackle network is illustrated in Fig. 3. Both electroplating and electroless depositions could be easily achieved on the patterned Au seed layer. For electroplating (Fig. 3a, left), the Au seed coated substrate was made the working electrode and a Cu plate was the counter electrode in a Cu plating bath containing copper sulphate (0.2 g ml^{-1}) and sulphuric acid (0.050 g ml^{-1}) solution and the thickness could be controlled by the deposition time and the applied voltage. For the electrode shown in Fig. 3b and c, the deposition was carried out with an applied voltage of 0.6 V for 45 s to result in a Cu network ~300 nm thick. The Cu metal was deposited selectively on Au such that regions devoid of Au were kept clear to result in a transparent electrode (Fig. 3b). Fig. 3c shows a highly interconnected Cu network formed by electroplating, further confirmed by XRD (ESI,

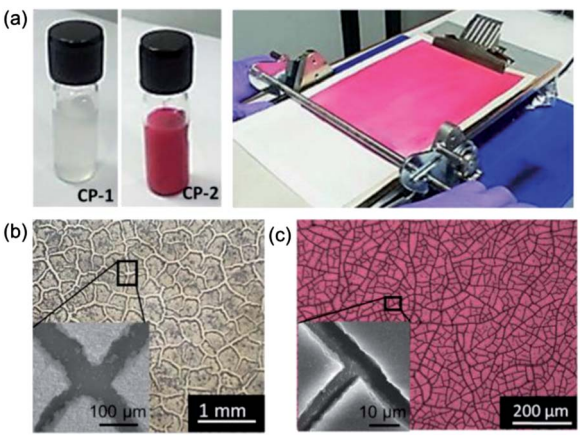

Fig. 1 Fabrication of crackle template: (a) crackle dispersions used in this study are commercially available, a wall paint containing colloidal SiO_2 (CP-1) and a cosmetic containing acrylic emulsion (CP-2). Both are amenable to rod coating. High magnification photographs along with SEM images (in insets) of crack network formed in CP-1 (b) and (c) CP-2.

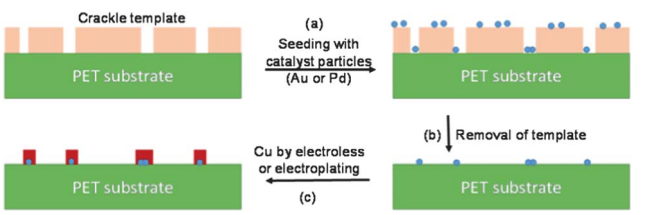

Fig. 2 Schematic showing Cu metal wire network based TCE fabrication using solution route. (a) Seeding of catalyst particles in the crackle grooves, (b) removal of cracked template, (c) Cu deposition by electroless method or by electroplating.

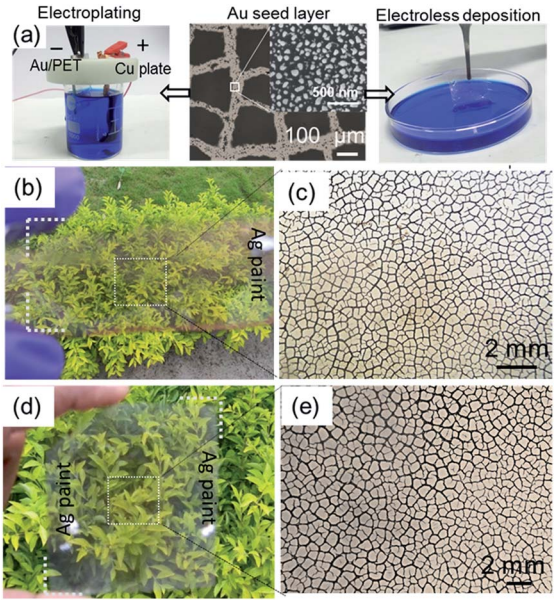

Fig. 3 (a) Cu deposition over Au seeds by electroless and electroplating methods. Photographs of the substrates electroplated (b) and electrolessly deposited (d) with Cu, and the respective magnified microscopic images are in (c) and (e).

Fig. S4†). In electroless deposition, the Au network containing substrate was dipped in a plating bath (copper : formaldehyde, 10 : 1) for different times without any external voltage and Cu networks of varying thicknesses were obtained (Fig. 3a, right). The photograph in Fig. 3d shows a transparent electrode obtained with electroless deposition with the network image in Fig. 3e. The network formed is continuous and extends over a large area (ESI, Fig. S5†).

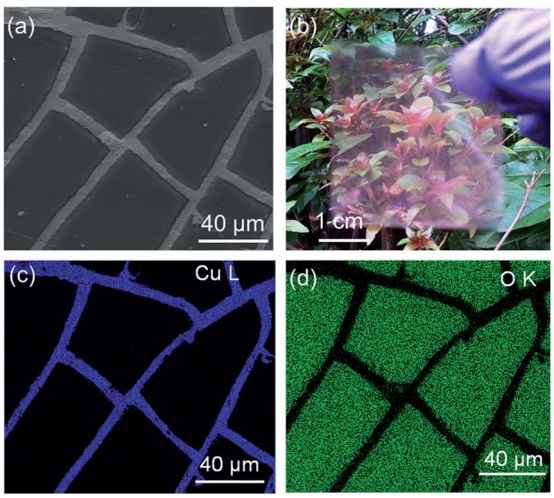

Fig. 4 (a) SEM image of Cu electrolessly deposited on Pd; (b) a photograph of a flowering plant as seen through a Cu wire network TCE. EDS maps corresponding to (c) Cu L and (d) O K for the SEM image in (a). In the O K map, the Cu network region is dark indicating no detectable surface oxidation, while the signal from the PET substrate may be seen from other regions.

The crackle network obtained in CP-2 was replicated with a Pd seed layer (Fig. 4a) by thermal decomposition of $PdCl_2$ dosed from solution and washing away the crackled layer with chloroform. The substrate was then dipped in an electroless plating bath wherein uniform coverage of Cu took place to give rise to a Cu wire network as shown in Fig. 4a. A view of the substrate carrying the network (Fig. 4b) clearly shows its transparency to the visible light. The presence of Cu over the Pd seed layer is confirmed by EDS mapping (Fig. 4c and d). As expected, the Pd seed layer gives very low signal as the layer is quite thin (ESI, Fig. S6†) and buried underneath. The Cu L signal clearly indicates that the surface is composed of Cu with no detectable signal from oxidation (see Fig. 4d).

Fig. 5a shows the transmittance spectra that are nearly flat and featureless over the entire visible region, even extending to the IR region (also see Fig. S7†). The flat transmittance is advantageous for display devices while transmittance in the IR range is useful for solar application. The transmittance at 550 nm is 70.2%, 68% and 74%, for Cu EP and ELD (referring to electroplating and electroless deposition, respectively) on the CP-1 pattern and Cu ELD on the CP-2 electrodes, respectively. The sheet resistance values were very low, ~0.3 (EP, CP-1), 1.3 (ELD, CP-1) and 3.8 $\Omega\,\square^{-1}$ (ELD, CP-2). In the case of EP, the deposited metal tends to closely pack with good electrical connectivity between the neighbouring grains. Under the experimental conditions employed, the thickness of Cu deposited is greater in case of EP (~300 nm) as compared to ELD (~100 nm). This resulted in a lower resistance for EP deposited electrodes as compared to ELD. In Fig. 5b, we compare the performance of our TCEs with Cu nanowire based TCEs reported in the literature (from both physical and solution processing). It is clear from the plot that the performance parameters obtained in this study compare well and are somewhat better than the values reported for solution processed TCEs. In solution processing, a small amount of non-specific deposition is unavoidable (ESI, Fig. S8†) which lowers the transmittance value. As is obvious, the physical deposition of Cu can be directly performed over the crackle template giving rise to a TCE with higher transmittance (ESI, Fig. S9†). However, resorting to physical deposition would be a big compromise on the cost and simplicity offered by solution processing.

Stability against oxidation is an important aspect of a Cu wire network based TCE, as many devices require annealing of the overlaid active layer at mild temperatures. This is done also to improve the coupling between the active layer and the electrode. We have examined this in detail, by heating a TCE (Cu ELD/PET) at 130 °C on a hot plate under ambient conditions while monitoring the variation in its resistance with time (see Fig. 6). As can be seen from Fig. 6a, the change in the resistance is very slow. Eventually, there was some oxygen uptake on the Cu wire surface (compare Fig. 6c with 4d). Thus, it took ~31 hours for resistance to increase by an order of magnitude. This observation is remarkable compared to literature results, where an order of magnitude increase in the sheet resistance in just a few hours is quite common upon heating to mild temperatures.[28] In some examples, Cu wires needed extra treatment such as passivation[27,29] or thermal annealing in vacuum.[32]

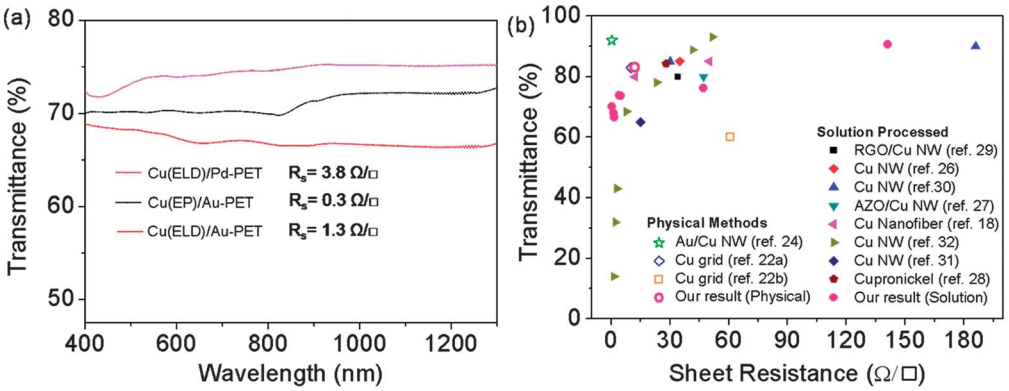

Fig. 5 (a) Transmittance spectra and resistance values of the various Cu wire network based TCEs; EP and ELD refer to electroplating and electroless deposition, respectively. The seed particle (Pd or Au) is indicated. Sheet resistance values are also shown. (b) Transmittance (at 550 nm) *versus* sheet resistance for the TCEs prepared in this study and their comparison with Cu based TCEs from the literature. Those produced by a physical method are shown with open symbols and those from solution processing are represented by solid symbols.

Hydrogen annealing above 300 °C is often adopted for obtaining good conductivity,[18] but it is not feasible in the case of flexible electrodes using substrates such as PET. The enhanced stability of our TCEs towards oxidation is understandable as these Cu wire networks are virtually devoid of crossbar junctions, found in TCEs prepared by depositing nanowire dispersions. Crossbar junctions may behave like hotspots with respect to oxidation. In our TCEs, the Cu wires are highly interconnected and the junctions are seamless (Fig. 4a) and therefore, the junction resistance is no longer a serious concern. This explains the enhanced stability of the TCE even at elevated temperatures. At room temperature, the TCE showed only 2% change in resistance over a period of 4 months. The relatively higher wire widths may also contribute to enhanced stability.[26]

We have explored the wetting behaviour of our Cu TCEs, which is another interesting aspect. A TCE used as a transparent heater, if hydrophobic, will have the advantage of self-cleaning. The hydrophilic nature of a TCE plays an important role at the interface with an electrolyte as in an electrochromic device. In either case, the back side being hydrophobic is clearly an advantage. The substrate, PET, used in this study does exhibit high water contact angles (~80°). An as-prepared Cu ELD/PET also exhibited a similar contact angle (see left inset in Fig. 6d), as the metal covered region is only a small fraction (~25%). In

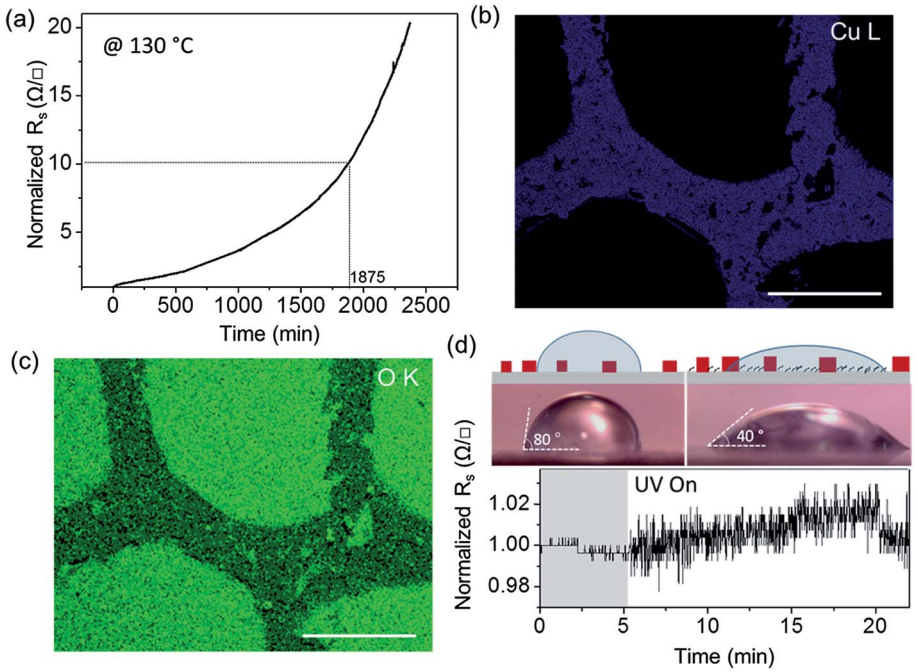

Fig. 6 Thermal oxidation stability: (a) variation in the normalized sheet resistance with time at 130 °C. (b) Cu L and (c) O K EDS maps at the end of the heat treatment. Scale bar 200 μm. (d) Variation in the normalized sheet resistance with time for another TCE, under UV–ozone treatment with the top insets showing water contact angle measurements before and after UV–ozone exposure.

order to decrease the contact angle, we resorted to treating the exposed PET regions with UV–ozone plasma for 10 min (at 4.6 mW cm^{-2} with an ozone level of 180 mg m^{-3}) which should enhance the wetting behaviour.[35] Following this treatment, the contact angle decreased to ~40° (see right inset in Fig. 6d). However, the resistance of the TCE was unchanged implying that the Cu wire network was practically unaffected.

Due to the extended interconnection between the wire networks without any junctions, the electrodes exhibit excellent flexibility. The bending of the electrode was performed at different bend radii followed by several bending cycles. The Cu wire network electrode prepared by ELD as well as EP did not show any significant change in resistance on bending to different radii from 12 mm to 2 mm and after release (Fig. 7a and b). The overall resistance of the electrodes was unaffected. The Cu wire network was subjected to several bending cycles as well, to test the mechanical stability of the electrode (Fig. 7d).

Conclusions

In this study, we have developed a solution based method to produce a large area TCE consisting of a Cu wire network on a flexible PET substrate. The Cu wire network was obtained by electroplating or by electrolessly coating Cu onto a sacrificial template hosting a crackled network. Pd or Au nanoparticles were used as seeds to grow Cu. We have employed commercially available, inexpensive colloidal dispersions which upon coating on PET and drying, spontaneously formed networks of crackles. Cu wire network TCEs were produced at two different length scales (wire widths ~10 and 100 μm) by choosing different crackle dispersions and optimising the coated layer thickness. The TCEs with broader wire networks may be of interest in large panel displays, while finer networks may be useful in touch screens and solar cells. The Cu TCEs produced in this study exhibit high transmittance (~67–75%) with low sheet resistance values (<5 Ω □$^{-1}$). With 141 Ω □$^{-1}$, we could achieve transmittance of ~90%. These values compare well with those from Cu TCEs reported in the literature based on solution processing. Large area (~A4 size) TCEs have also been made by this method. Importantly here, the Cu wire networks were highly interconnected in a single plane with no crossbar junctions, leading to extreme stability towards oxidation in air, even at elevated temperatures. The TCEs were also found to be highly flexible, a property borrowed from the PET substrate, but with no appreciable change in resistance upon increasing the number of bending cycles. The water wetting properties of the TCE could be switched from hydrophobic to hydrophilic by UV–ozone treatment, importantly, without changing the resistance. Being a solution process, the method should be of high significance for the optoelectronics industry. Future efforts will include solution based processing without the use of metal catalysts.[36]

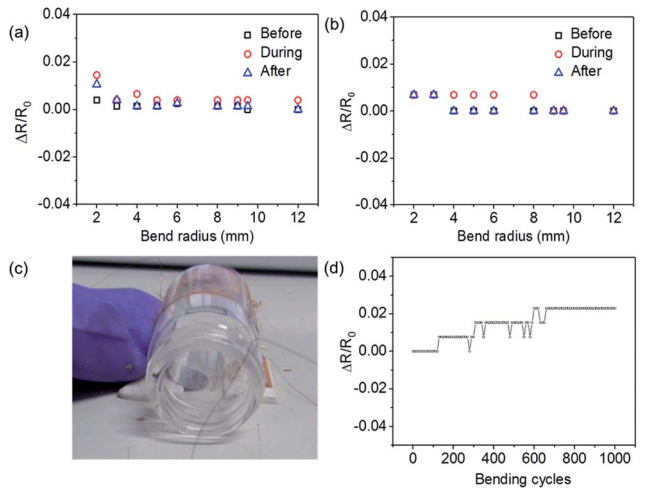

Fig. 7 Flexibility tests. Variation in the normalised sheet resistance as Cu ELD/PET (a) and Cu EP/PET (b) were bent to different radii. (c) A photograph showing a TCE bent around a vial of diameter 12 mm. (d) Variation in the normalised sheet resistance with a large number of bending cycles with a bending radius of 4 mm. Every 10th data point is shown for clarity.

Experimental

Fabrication of crack template by rod coating

A commercial SiO_2 nanoparticle dispersion termed here as CP-1 is a crackle paint (Premium Coatings & Chemicals, India) and CP-2 is a water based acrylic resin sold as a cosmetic product (Ming Ni Cosmetics Co., Guangzhou, China). Typically, CP-1 or CP-2 dispersion in diluter (0.3 g ml^{-1}) was rigorously ultrasonicated for 30 min. The dispersion was left overnight in an air-tight bottle. The suspended solution was extracted as needed and ultrasonicated prior to drop, spin or rod coating on a polyethylene terephthalate (PET) substrate (~80 μm thick). The substrate was then left to dry in air while a crackle network pattern formed spontaneously in the coated layer. The crackle precursor formulations (CP-1 and CP-2) contain film forming agents that enable smooth and uniform coating of the template over large areas as shown in Fig. 1. Moreover, the solvents present in the CP impart additional qualities. For example, ethyl acetate improves the spreading while pentyl acetate helps in levelling off the dispersion.

Fabrication of Cu wire network based TCE

For metal deposition by electroplating (EP) and electroless (ELD) methods, a thin Au layer was deposited over the crackled network by a sputtering technique. This acts as a seed layer for further deposition of copper by EP and ELD. The copper electroplating solution is prepared by dissolving 230 g of copper sulphate solution in 1 l of water, and to that 140 ml of conc. H_2SO_4 was added. To electroplate Cu over the Au network on PET, the substrate with the Ag contact was taken as the cathode and a Cu foil as the anode. By applying a potential between the two electrodes, Cu was deposited over the Au seed network and the reaction was stopped after obtaining the required thickness.

The Cu plating bath used for the electroless deposition was composed of 3 g of $CuSO_4$, and 14 g of sodium potassium tartrate mixed with 4 g of NaOH in 100 ml of distilled water

(solution A). Solution B was an aqueous formaldehyde solution (37.2 wt%). Solutions A and B were mixed in a 10 : 1 ratio. To deposit Cu, the Au seed network on PET was immersed in the freshly prepared mixture for 10 min at room temperature. The plating process was stopped by removing the sample and rinsing with distilled water.

Characterization of transparent conducting electrode

Transmittance was measured using a Perkin-Elmer Lambda 900 UV/visible/near-IR spectrophotometer. Sheet resistance was measured using a 4-Point Probe Station (Techno Science Instruments, India). SEM was carried out using a Nova NanoSEM 600 instrument (FEI Co., The Netherlands). Energy-dispersive spectroscopy (EDS) analysis was performed with an EDAX Genesis instrument (Mahwah, NJ) attached to the SEM column. Electroplating of Cu over the seed layer was performed using an electrochemical station (CH-Instruments 650, Austin, TX, USA). A Wyko NT9100 Optical Profiling System (Bruker, USA) was used for height and depth measurements. Flexibility tests were performed using a custom designed set up. UV–ozone treatment of the fabricated TCEs was performed using Bioforce ProCleaner equipment.

Flexibility test

The flexibility tests were performed for Cu/PET based electrodes using a custom designed setup with one side fixed while the other was kept movable using a screw gauge attachment. Silver epoxy adhesive was used for making contact pads on both sides of the Cu/PET electrode. The resistance change during bending at different bending radii was recorded through a digital multimeter (Test Link, India) interfaced with a computer using DMM viewer software. The stability of the electrodes over 1000 bending cycles (sinusoidal) was tested at a rate of 0.05 Hz with a bending radius of 4 mm.

Acknowledgements

The authors are grateful to Professor C. N. R. Rao for his encouragement. The financial support from the Department of Science and Technology, Government of India, is gratefully acknowledged. S. K. and K. D. M. R. acknowledge DST-INSPIRE and UGC, respectively, for fellowships.

Notes and references

1 C. G. Granqvist, *Sol. Energy Mater. Sol. Cells*, 2007, **91**, 1529.
2 M. Katayama, *Thin Solid Films*, 1999, **341**, 140.
3 Y. Yang, *et al.*, *Adv. Mater.*, 2004, **16**, 321.
4 U. Betz, M. K. Olsson, J. Marthy, M. F. Escola and F. Atamny, *Surf. Coat. Technol.*, 2006, **200**, 5751.
5 C. Y. Lim, J. K. Park, Y. H. Kim and J. I. Han, *Journal of International Council on Electrical Engineering*, 2012, **2**, 237.
6 O. J. Gregory, Q. Luo and E. E. Crisman, *Thin Solid Films*, 2002, **406**, 286.
7 Y. Gassenbauer and A. Klein, *J. Phys. Chem. B*, 2006, **110**, 4793.
8 R. M. Pasquarelli, D. S. Ginley and R. O'Hayre, *Chem. Soc. Rev.*, 2011, **40**, 5406.
9 S. Bae, *et al.*, *Nat. Nanotechnol.*, 2010, **5**, 574.
10 J. Zhang, P. A. Hu, X. Wang, Z. Wang, D. Liu, B. Yangc and W. Caoc, *J. Mater. Chem.*, 2012, **22**, 18283.
11 Q. Zheng, B. Zhang, X. Lin, X. Shen, N. Yousefi, Z. D. Huang, Z. Lia and J. K. Kim, *J. Mater. Chem.*, 2012, **22**, 25072.
12 C. M. Aguirre, S. Auvray, S. Pigeon, R. Isquierdo, P. Desjardins and R. Martel, *Appl. Phys. Lett.*, 2006, **88**, 183104.
13 D. S. Hecht, L. Hu and G. Irvin, *Adv. Mater.*, 2011, **23**, 1482.
14 R. Wang, J. Sun, L. Gao and J. Zhang, *ACS Nano*, 2010, **4**, 4890.
15 H. Wu, *et al.*, *Nat. Nanotechnol.*, 2013, **8**, 421.
16 A. Kim, Y. Won, K. Woo, C. H. Kim and J. Moon, *ACS Nano*, 2013, **7**, 1081.
17 J. Y. Lee, S. T. Connor, Y. Cui and P. Peumans, *Nano Lett.*, 2008, **8**, 689.
18 H. Wu, L. Hu, M. W. Rowell, D. Kong, J. J. Cha, J. R. McDonough, J. Zhu, Y. Yang, M. D. McGehee and Y. Cui, *Nano Lett.*, 2010, **10**, 4242.
19 D. S. Ghosh, T. L. Chen and V. Pruneri, *Appl. Phys. Lett.*, 2010, **96**, 091106.
20 A. Reina, *et al.*, *Nano Lett.*, 2008, **9**, 30.
21 D. R. Lide, *CRC handbook of chemistry and physics*, CRC press, Boca Raton, FL, 85th edn, 2004.
22 (*a*) M. G. Kang, M. S. Kim, J. Kim and L. J. Guo, *Adv. Mater.*, 2008, **20**, 4408; (*b*) D. S. Ghosh, R. Betancur, T. L. Chen, V. Pruneri and J. Martorell, *Sol. Energy Mater. Sol. Cells*, 2011, **95**, 1228.
23 R. Gupta and G. U. Kulkarni, *ACS Appl. Mater. Interfaces*, 2013, **5**, 730.
24 P. Hsu, S. Wang, H. Wu, V. Narasimhan, D. Kong, H. R. Lee and Y. Cui, *Nat. Commun.*, 2013, DOI: 10.1038/ncomms3522.
25 C. Sachse, N. Weib, N. Gaponik, L. M. Meskamp, A. Eychmuller and K. Leo, *Adv. Energy Mater.*, 2013, DOI: 10.1002/aenm.201300737.
26 D. Zhang, R. Wang, M. Wen, *et al.*, *J. Am. Chem. Soc.*, 2012, **134**, 14283.
27 P. C. Hsu, *et al.*, *ACS Nano*, 2012, **6**, 5150.
28 A. R. Rathmell, M. Nguyen, M. Chi and B. J. Wiley, *Nano Lett.*, 2012, **12**, 3193.
29 I. N. Kholmanov, *et al.*, *ACS Nano*, 2013, **7**, 1811.
30 A. R. Rathmell, S. M. Bergin, Y. L. Hua, Z. Y. Li and B. J. Wiley, *Adv. Mater.*, 2010, **22**, 3558.
31 A. R. Rathmell and B. J. Wiley, *Adv. Mater.*, 2011, **23**, 4798.
32 H. Guo, N. Lin, *et al.*, *Sci. Rep.*, 2013, DOI: 10.1038/srep02323.
33 H. Kim, *et al.*, *J. Appl. Phys.*, 1999, **86**, 6451–6461.
34 M. Manceau, D. Angmo, M. Jørgensen and F. C. Krebs, *Org. Electron.*, 2011, **12**, 566.
35 I. K. Moon, J. I. Kim, H. Lee, K. Hur, W. C. Kim and H. Lee, *Sci. Rep.*, 2013, **3**, 1112, DOI: 10.1038/srep01112.
36 W. P. Dow, G. L. Liao, S. E. Huang and S. W. Chen, *J. Mater. Chem.*, 2010, **20**, 3600.

